Structural Change in Li and Na Aluminophosphate Glasses: Evidence of a "Structural Mixed Alkali Effect"

D. Viviani,[†] A. Faivre,*[,†] C. Levelut,[†] and M. Smaïhi[‡]

Laboratoire des Colloïdes, Verres et Nanomatériaux, UMR/CNRS 5587, Université de Montpellier II - Place E. Bataillon, 34095 Montpellier Cedex 5, France, and Institut Européen des Membranes, UMR/CNRS 5635, 1919 Route de Mende, 34293 Montpellier Cedex 5, France

Received: October 12, 2005; In Final Form: February 10, 2006

The short- and long-range structure of a series of single and mixed aluminophosphate glasses with the general composition [xNa$_2$O ($46 - x$)Li$_2$O], [yAl$_2$O$_3$ ($54 - y$)P$_2$O$_5$] is analyzed using ^{31}P and ^{27}Al magic-angle spinning (MAS) NMR as well as small-angle X-ray scattering. These series of glasses allow analyzing both the effect of alumina incorporation in these glasses, for small alumina content ($y = 0$, 4, 8), and the structural changes associated with the so-called mixed alkali effect ($x = 0$, 11.5, 23, 34.5, 46). Our results indicate that aluminum is mainly octahedrally coordinated in these glasses and that there is most likely some segregation of the Al(OP)$_6$ species. In the pure phosphate glasses, we observe a "classical" continuous variation of the structural properties with the relative alkali content, but in the aluminophosphate, both local and long-range structural results reveal for the first time some nonlinear change as a function of the relative alkali content.

Introduction

The mixed alkali effect (MAE) corresponds to the nonlinear variation of certain physical properties with the relative alkali content in glasses containing two or more different types of alkali ions. This MAE is known to be more pronounced for properties related to ionic mobility.[1−3] In the past few years, numerous studies have been devoted to the investigation of the structural origin of the MAE. Different extended X-ray absorption fine structure (EXAFS) experiments and molecular dynamics simulations have suggested that each type of cation is located in rather distinct local sites in mixed alkali glasses.[4−6] In mixed lithium sodium silicate glasses, Gee et al.[7,8] observed monotonic compositional dependences of alkali NMR chemical shifts, suggesting intimate mixing of Li and Na species, while silicon alkali rotational echo double resonance (REDOR) difference NMR experiments fail to give any evidence for like cation clustering. Their results also indicate that local order is preserved around each alkali for different alkali mixtures. Park et al.[9] investigated the structure of Li−K silicate glasses by molecular dynamics simulation and showed that the environment of each kind of alkali differs from that of the other type, regardless of whether in single or mixed alkali glasses. In mixed alkali phosphate glasses as well, diffraction experiments in combination with reverse Monte Carlo (RMC) simulations showed that the cations are randomly distributed between the phosphate chains and that the local environments for the two types of cations are significantly different.[10,11] These studies led to the same kind of conclusions: first of all, in mixed alkali glasses, the different alkali ions are statistically mixed within an overall fairly homogeneous spatial distribution, and second, local order is preserved around each type of alkali.

These last conclusions served as the basis for the recent explanations of the MAE. The dynamic structure model[12−14] as well as the random distribution model[10] invoke alkali site mismatches (different structural arrangements around different alkali elements) and percolation effects between these different sites to explain the slowing down of the ion mobility in mixed alkali glasses.

To better understand the role of the network on the site mismatches, we recently investigated the influence of alumina incorporation on the MAE in Na−Li phosphate glasses containing a global alkali ratio of 46 mol %. We showed that the direct current (dc) conductivity minimum characteristic of the MAE decreases and almost disappears as Al_2O_3 is added to mixed phosphate glasses. The dc conductivity of the single alkali glasses is almost not affected by Al_2O_3 addition. Dielectric relaxation characteristics also change with Al_2O_3 concentration in mixed glasses and not in single ones. On the other hand, the mixed alkali peak measured using mechanical relaxation spectrometry appears to be almost not affected by the presence of Al_2O_3.[15]

In this paper, we investigate the structural changes associated with the addition of alumina in three series of sodium−lithium aluminophosphate glasses, that have already been analyzed by dielectric and mechanical spectroscopies.[15] They all contain the same total alkali ratio (46 mol %), but they have three different Al_2O_3 contents (0, 4, and 8 mol %). The short-range structure of these glasses is analyzed using ^{31}P and ^{27}Al magic-angle spinning (MAS) NMR. On the other hand, small-angle X-ray scattering (SAXS) allows probing of the structure on a more extended range.

Experimental Procedure

The synthesis of the 15 lithium and sodium aluminophosphate glasses (see Table 1 for details) has been previously reported.[15] The glass compositions underwent chemical analysis at the "Laboratoire Central d'Analyse du CNRS de Vernaison" and are also presented in Table 1. Differences between nominal (calculated from the introduced compounds) and analyzed

* Corresponding author. Phone: +33.4.67.14.32.84. Fax: +33.4.67.54.48.01. E-mail: alfaivre@univ-montp2.fr.
[†] UMR/CNRS 5587.
[‡] UMR/CNRS 5635.

10.1021/jp055835g CCC: $33.50
Published on Web 03/17/2006

TABLE 1: Nominal (Calculated from the Introduced Compounds) and Analyzed Compositions (± 0.5 mol %) of the Aluminophosphate Glasses Synthesized for This Study

nominal glass composition	mol % Na_2O	mol % Li_2O	mol % Al_2O_3	mol % P_2O_5
$0.46Li_2O\ 0.54P_2O_5$	0	49.6	0	50.4
$0.345Li_2O\ 0.115Na_2O\ 0.54P_2O_5$	14.1	33.3	0	52.6
$0.23Li_2O\ 0.23Na_2O\ 0.54P_2O_5$	23.9	22.4	0	53.7
$0.115Li_2O\ 0.345Na_2O\ 0.54P_2O_5$	35	11.2	0	53.8
$0.46Na_2O\ 0.54P_2O_5$	50.3	0	0	49.7
$0.46Li_2O\ 0.04Al_2O_3\ 0.5P_2O_5$	0	45.1	3.4	51.5
$0.345Li_2O\ 0.115Na_2O\ 0.04Al_2O_3\ 0.5P_2O_5$	14.2	33	4.1	48.7
$0.23Li_2O\ 0.23Na_2O\ 0.04Al_2O_3\ 0.5P_2O_5$	24.2	22.3	4	49.5
$0.115Li_2O\ 0.345Na_2O\ 0.04Al_2O_3\ 0.5P_2O_5$	34.5	11.5	4	50
$0.46Na_2O\ 0.04Al_2O_3\ 0.5P_2O_5$	45	0	4	51
$0.46Li_2O\ 0.08Al_2O_3\ 0.46P_2O_5$	0	46.7	6.5	46.8
$0.345Li_2O\ 0.115Na_2O\ 0.08Al_2O_3\ 0.46P_2O_5$	12.9	32.3	7.9	46.8
$0.23Li_2O\ 0.23Na_2O\ 0.08Al_2O_3\ 0.46P_2O_5$	23.5	22.2	7.8	46.6
$0.115Li_2O\ 0.345Na_2O\ 0.08Al_2O_3\ 0.46P_2O_5$	34.8	11.1	7.8	46.3
$0.46Na_2O\ 0.08Al_2O_3\ 0.46P_2O_5$	46	0	7.6	46.3

compositions are lower in aluminophosphate glasses than in pure phosphate glasses and are always lower than 6% for all species. All samples gave a broad, featureless X-ray diffraction pattern, confirming the amorphous nature of the samples. The glass transition temperature (Tg) of each glass was determined using differential scanning calorimetry (Setaram TG/DSC Labsys-1600) at a heating rate of 5 K/min and has been presented elsewhere.[15]

NMR. All MAS solid state NMR spectra were acquired using a Bruker Avance 400 solid state spectrometer. The resonance frequencies of ^{27}Al and ^{31}P were 104.26 and 161.92 MHz, respectively. The powder samples were filled into 4 mm diameter zirconia rotors. Quantitative solid state ^{27}Al MAS NMR is difficult for a number of reasons related to the quadrupolar nature of this nucleus. To achieve uniform excitation across the range of aluminum environments, very short pulses of 1 μs duration (corresponding to approximately a $\pi/12$ flip angle) were used. The number of acquisitions ranged from 500 to 1000 with a 1s repetition rate. Magic-angle spinning was set at 10 kHz in order to ensure complete separation of sideband intensity from the central transition. ^{31}P MAS NMR spectra were acquired using a 1.5 μs pulse width (corresponding to a $\pi/6$ flip angle) with a 5 s repetition rate and employing magic-angle spinning at 10 kHz; 100−500 scans were accumulated. ^{27}Al and ^{31}P chemical shifts were referenced to 1% aqueous $Al(H_2O)_6^{3+}$ solution and 85% H_3PO_4, respectively.

SAXS. The small-angle X-ray measurements were carried out on the D2AM experimental setup of the European Synchrotron Radiation Facility (ESRF) in Grenoble, France. The measurements were performed on small plates of about 1 mm thickness, using an incident energy of 15 keV, allowing wave vectors ranging between 0.2 and 10 nm^{-1} to be probed. Accumulation times were of 200 s, and data were collected using a CCD camera. Radial integration and corrections from the variations of the incident flux, from the background scattering and cosmic rays, have been performed in the usual way, as well as normalization to the absorption of the sample. The scattered intensity was converted to absolute values, electron units per $0.46[xNa_2O\ (1-x)Li_2O]$, $0.54[yAl_2O_3\ (1-y)P_2O_5]$ composition unit, by scaling the data to the measured signal obtained with water. We assumed a value of 6.37 eu per H_2O molecule, which is almost constant from $q = 3$ to 7 nm^{-1}.[16] The probable error of the conversion factor is 4%.

Results

^{31}P MAS NMR. Phosphate tetrahedra, like silicate tetrahedra, can be described by their number of bridging oxygen (BO) and nonbridging oxygen (NBO) atoms. The standard notation Q^n identifies the number ($n = 0, 1, \ldots, 4$) of BO atoms per tetrahedron. Figure 1 shows the ^{31}P MAS NMR spectra of the mixed Na−Li phosphate glass series (0 mol % Al_2O_3). A central peak can be clearly observed around −20 ppm for all compositions. This isotropic chemical shift has been attributed in the literature to Q^2 phosphate sites,[17−19] corresponding to P tetrahedra with two BO. The structure of the mixed phosphate glasses can consequently be seen as being essentially constituted of long phosphate chains, which is in agreement with the almost metaphosphate composition. Other small resonances are observed for some compositions. The single lithium phosphate glass spectrum exhibits a small peak at an isotropic chemical shift of −4.8 ppm, which is difficult to assign. The three mixed Na−Li phosphate glasses exhibit two small contributions around −35 ppm and around −10 ppm, which have been respectively attributed to the presence of Q^3 and Q^1 phosphate sites.[19] Assuming a Gaussian line shape for each resonance peak, spectra were deconvoluted using an appropriate number of overlapping Gaussians. The amplitude of the main peak (associated with Q^2 species) is reported in Table 2 as well as its chemical shift and its full width at half-maximum (fwhm). Considering Van Wazer relationships describing, for binary alkali phosphate glasses, the tetrahedral site distribution as a function of composition,[20] one can calculate a "theoretical" Q^n tetrahedral distribution. Since quantitative measurements of the site population obtained from NMR are in excellent agreement with the

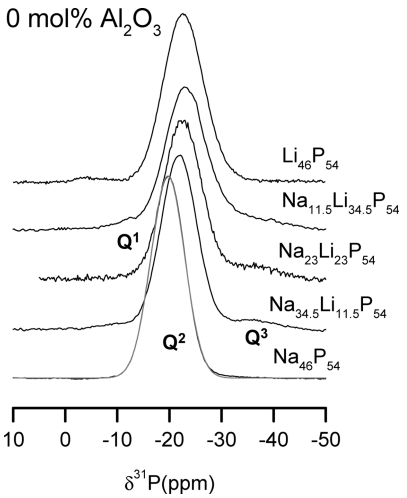

Figure 1. ^{31}P MAS NMR spectra (black lines) of the $0.46[xNa_2O\ (1-x)Li_2O]$, $0.54[P_2O_5]$ glass series. Gray lines correspond to fit and Gaussian deconvolution.

TABLE 2: ^{31}P MAS NMR Spectral Parameters for the 0.46[xNa$_2$O (1 − x)Li$_2$O], 0.54[P$_2$O$_5$] Glass Series and Comparison to the Relative Content of the Different Q^n Species Calculated Using the Van Wazer Equation[20]

nominal composition	$Li_{46}P_{54}$	$Na_{11.5}Li_{34.5}P_{54}$	$Na_{23}Li_{23}P_{54}$	$Na_{34.5}Li_{11.5}P_{54}$	$Na_{46}P_{54}$
measured composition	$Li_{49.6}P_{50.4}$	$Na_{14.1}Li_{33.3}P_{52.6}$	$Na_{23.9}Li_{22.4}P_{53.7}$	$Na_{35}Li_{11.2}P_{53.8}$	$Na_{50.3}P_{49.7}$
Q^2 δ_{iso}	-22.7 ± 0.2	-23.1 ± 0.2	-22.4 ± 0.2	-21.8 ± 0.2	-19.7 ± 0.2
Q^2 fwhm	7.7 ± 0.1	7.8 ± 0.1	7.4 ± 0.1	6.9 ± 0.1	6.5 ± 0.1
%Q^2 NMR	98.6 ± 3	85 ± 3	89.6 ± 3	91.6 ± 3	100 ± 3
%Q^2 Van Wazer	98 ± 2	90 ± 2	86 ± 2	86 ± 2	99 ± 2
%Q^3 NMR	0 ± 3	11 ± 3	10.4 ± 3	6.1 ± 3	0 ± 3
%Q^3 Van Wazer	2 ± 2	10 ± 2	14 ± 2	14 ± 2	0 ± 2
%Q^1 NMR	0 ± 3	4 ± 3	0 ± 3	2.3 ± 3	0 ± 3
%Q^1 Van Wazer	0 ± 2	0 ± 2	0 ± 2	0 ± 2	1 ± 2

Van Wazer equation for sodium metaphosphate glasses,[21] theoretical Q^1, Q^2, and Q^3 tetrahedral concentrations were calculated from the Van Wazer equation for the Na−Li phosphate glasses analyzed here (Table 2). A very good agreement has been found for the single Li or Na phosphate glasses, whose actual composition is closer to the metaphosphate composition. The differences observed for mixed glasses are bigger, up to 6.5%, but can be attributed to NMR and composition error bars. For ultraphosphate glasses, Van Wazer assumptions imply the absence of Q^1 tetrahedra that we observe experimentally for two compositions (Table 2). We could explain our observation by assuming a disproportionation reaction, often observed in silicate glasses:

$$2Q^2 \leftrightarrow Q^1 + Q^3$$

Such a site disproportionation reaction has however hardly ever been reported in ultraphosphate glasses.[21] It should be noted that the presence of Q^3 phosphate sites observed for mixed alkali glasses and their absence for the single alkali glasses (Table 2) has to be linked to the difference between the nominal and the experimentally measured glass composition, and not to a possible "mixed alkali effect" on the Q^n site distributions. The single alkali glasses indeed have a composition further than the nominal composition and close to metaphosphate glasses (Table 1). The absence of Q^3 phosphate sites in these single alkali glasses is predicted by the Van Wazer equation (Table 2) when experimentally measured compositions are used.

Figure 1 and Table 2 also show that, for these phosphate glasses, the Q^2 chemical shift becomes progressively less shielded when increasing the Na/Li ratio. This shifting is not linear with the relative alkali ratio, as was observed by Sato et al.[22] in Na−Li metaphosphate glasses. The nonlinearity we observe in Table 2 is again most likely due to the difference between the nominal and analyzed composition of our samples. The progressive shielding of phosphorus Q^2 chemical shift as the cation electronegativity increases has also been observed in numerous alkali and alkaline earth metaphosphate glasses.[23] This indicates that the P−O bond strength within the tetrahedron decreases as the external alkali oxygen bond strength increases.

The Q^2 peak breaths (fwhm) also exhibit an almost linear decrease when increasing the [Na]/[Na + Li] ratio (Table 2). The fwhm breadths of the pure Na−Li phosphate glasses are slightly narrower than what Sato et al. found in Na−Li metaphosphate[22] and closer to what is found in corresponding crystalline phosphate (3−7 ppm).[17] As already observed in different mixed alkali glasses, this continuous variation of the Q^2 peak position and width with the [Na]/[Na + Li] ratio indicates that Na and Li ions are mixed on an atomic scale.

The analysis of the ^{31}P MAS NMR spectra obtained for the Na−Li aluminophosphate glass series is more complicated due to the convolution of different resonance peaks. Spectra are presented in Figures 2 and 3, respectively, for glass series with 4 and 8 mol % alumina. Presumably, each resonance peak corresponds to a phosphate tetrahedron with different atomic neighbors in its second coordination sphere. Adding alumina to the phosphate glasses while keeping the total alkali ratio constant indeed induces a new type of bonding: POAl linkages progressively replace POP bonds. To distinguish between the different kinds of PO_4 tetrahedra, we will adopt a new Q^n_m notation, introduced by Grimmer and Wolf,[24] for the phosphorus environment. The subscript n identifies now the number of bridging oxygen atoms to another P atom per tetrahedron, and

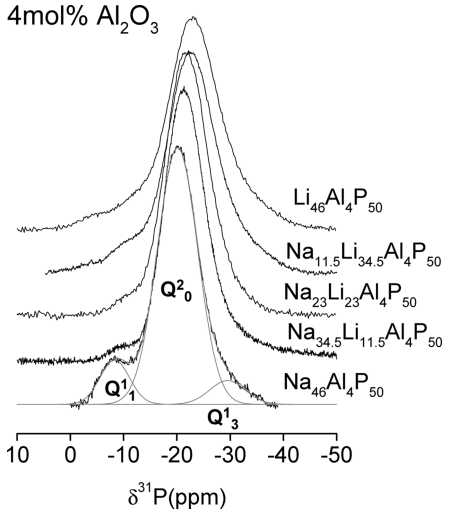

Figure 2. ^{31}P MAS NMR spectra (black lines) of the 0.46[xNa$_2$O (1 − x)Li$_2$O], 0.50[P$_2$O$_5$], 0.04[Al$_2$O$_3$] glass series. Gray lines correspond to fit and Gaussian deconvolution.

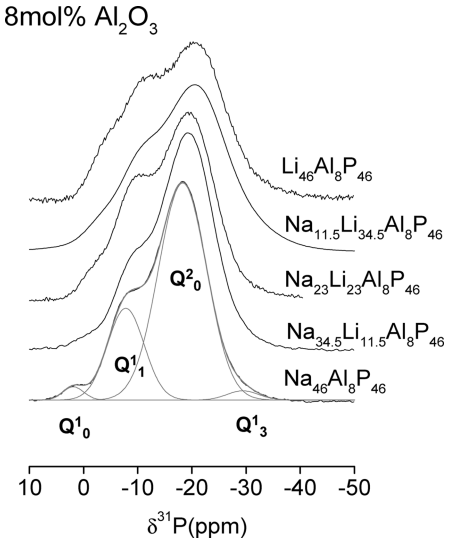

Figure 3. ^{31}P MAS NMR spectra (black lines) of the 0.46[xNa$_2$O (1 − x)Li$_2$O], 0.46[P$_2$O$_5$], 0.08[Al$_2$O$_3$] glass series. Gray lines correspond to fit and Gaussian deconvolution.

TABLE 3: Deconvolution Parameters Obtained from ^{31}P MAS NMR Spectra for the Two Aluminophosphate Glass Series Presented in Figures 2 and 3[a]

	Q^1_3			Q^2_0			Q^1_1			Q^1_0		
	ppm	fwhm	(%)	ppm	fwhm	(%)	ppm	fwhm	(%)	ppm	fwhm	(%)
$Li_{45.1}P_{51.5}Al_{3.4}$	−28.0	13.6	31	−22.5	8.3	59	−12.2	6.0	6	−5.1	6.8	4
$Na_{14.2}Li_{33}P_{48.7}Al_{4.1}$	−28.9	11.9	24	−22.1	8.1	66	−12.0	6.5	8	−3.1	6.6	2
$Na_{24.2}Li_{22.3}P_{49.5}Al_4$	−29.0	7.1	7	−21.5	7.6	88	−10.5	5.8	5			
$Na_{34.5}Li_{11.5}P_{50}Al_4$	−27.8	14.4	22	−21.2	7.1	77	−9.3	3.5	2			
$Na_{46}P_{51}Al_4$	−29.5	6.7	7	−20.1	7.6	83	−8.3	5.5	10			
$Li_{46.7}P_{46.8}Al_{6.5}$	−35.7	11.4	3	−20.5	11.1	65	−10.3	6.6	21	−3.9	5.5	10
$Na_{12.9}Li_{32.3}P_{46.8}Al_{7.9}$	−32.8	10.3	5	−20.5	11.3	70	−10.4	6.8	16	−4.0	8.3	9
$Na_{23.5}Li_{22.2}P_{46.6}Al_{7.8}$	−32.3	10.2	3	−19.5	9.3	65	−9.0	7	28	−1.5	4.7	4
$Na_{34.8}Li_{11.1}P_{46.3}Al_{7.8}$	−30.0	8.6	3	−19.3	9.0	73	−9.0	6.9	21	−0.4	6.2	3
$Na_{46}P_{46.3}Al_{7.6}$	−29.4	5.8	2	−18.3	8.9	73	−7.8	6.8	23	1.9	4	2

[a] Estimated errors are ±0.5 ppm on the peak positions, ±0.6 ppm on the fwhm, and ±3% on the area ratio.

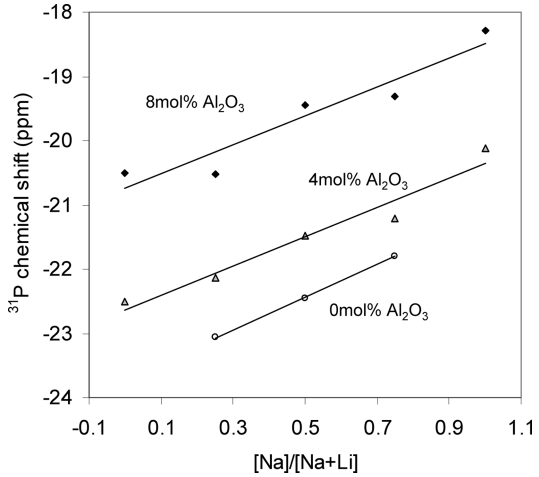

Figure 4. Variation of the ^{31}P MAS NMR chemical shift of the main Q^2 contribution as a function of the relative alkali content for the three aluminophosphate series. The points corresponding to the single Li and Na pure phosphate glasses are not shown, because their measured phosphate content is too far from the other glasses (see Table 1 for details).

the subscript *m* identifies the number of bridging oxygen atoms to an Al atom per tetrahedron. ^{31}P chemical shifts have been reported in the literature for sodium aluminophosphate crystals[24,25] and for sodium phosphate glass:[23,26] assigments to Q^n_m sites are well summarized and analyzed in ref 27.

Table 3 summarizes the peak position, fwhm, and relative intensity for the different Gaussian lines used to obtain converging fits of the spectra presented in Figures 2 and 3. Given the number of possible Q^n_m sites and the degree of overlap of the resonances, satisfactory fits can be obtained with variation of the position and intensity of the different Gaussians, as well as the number of Gaussians used. The accuracy of this analysis is somewhat limited, and we will consequently discuss only unambiguous results.

All spectra clearly reveal a resonance peak with a chemical shift around −20 ppm, which can easily be assigned to Q^2_0 phosphate tetrahedra. As observed in Figure 4, the "usual" shielding of this principal isotropic chemical shift with increasing [Na]/[Na + Li] ratio is weakly affected by the addition of alumina. However, replacement of P by Al involves a less shielded chemical shift, as observed in Figure 4. This can be explained by the electronegativity difference between P and Al, which implies more covalent P−O bonds with increasing Al/P ratio. The fwhm of the resonance band associated with Q^2_0 slightly increases with the addition of alumina, with this increase being more important in the 8 mol % aluminophosphate glasses than in the 4 mol % ones. This may indicate that the distribution of the P−O−P angles gets larger as alumina is added and that the type of second next-nearest neighbor is probably more distributed.

As observed in Figures 2 and 3, shoulders develop around the principal Q^2_0 peak, with this effect being more pronounced for the 8 mol % aluminophosphate glasses. The attribution of these secondary chemical shifts is more complicated. On the high-frequency side, a shoulder is clearly visible for the 0.46-(Na_2O) 0.50(P_2O_5) 0.04(Al_2O_3) glass around −8 ppm (see Figure 2). This shoulder becomes more negative when increasing the Al/P ratio for this single alkali sodium aluminophosphate glass (see Figure 3 and Table 3). This −8 ppm peak has been assigned to the Q^1_1 aluminophosphate group that forms when POAl progressively replaces POP linkages.[28] It has to be quoted that the fwhm of these peaks is rather small (5.5 and 6.8 ppm) compared to what Brow et al. obtained (around 20 ppm). When the [Na]/[Na + Li] ratio in the glasses containing 4 and 8 mol % Al_2O_3 is decreased, the peak associated with Q^1_1 becomes progressively more shielded. This is again consistent with the increase in electronegativity of the modifying cations. Figures 2 and 3 also clearly show that this Q^1_1 contribution increases with alumina.

On the high-frequency side, a second low peak can be easily detected around 2 ppm in the single Na aluminophospahte glass with 8 mol % Al_2O_3. This peak has also been observed in other sodium aluminophosphate glasses and assigned to a Q^1_0 P tetrahedron.[28] As the [Na]/[Na + Li] ratio decreases in the 8 mol % aluminophosphate glasses, this peak becomes more shielded (Table 3). It has to be noted that this contribution is not observable in the Na rich aluminophosphate glasses with 4 mol % Al_2O_3 and that its amplitude increases with decreasing Na/Li ratio.

On the low-frequency side, an additional band, centered around −30 ppm in the single Na aluminophosphate glasses, is necessary to obtain reasonable fits (Table 3). This contribution is not easily detectable in Figures 2 and 3, and its attribution is difficult. It could be assigned either to Q^2_1 (that has never been observed in the literature) or to Q^1_3 tetrahedra (see Figure 2 of Brow's paper[27]). This peak becomes much more shielded as the [Na]/[Na + Li] ratio decreases in the aluminophosphate glasses with 8 mol % Al_2O_3 (see Table 3) but remains almost constant in the aluminophosphate glasses with 4 mol % Al_2O_3. This peak fwhm varies also significantly and not very smoothly as the [Na]/[Na + Li] ratio decreases. These results may again suggest that, in the Li rich glasses, an additional contribution could be added to fit the data. However, due to the convolution between these high-frequency contributions and the main Q^2_0 contribution, such fits would not be valuable. What is however

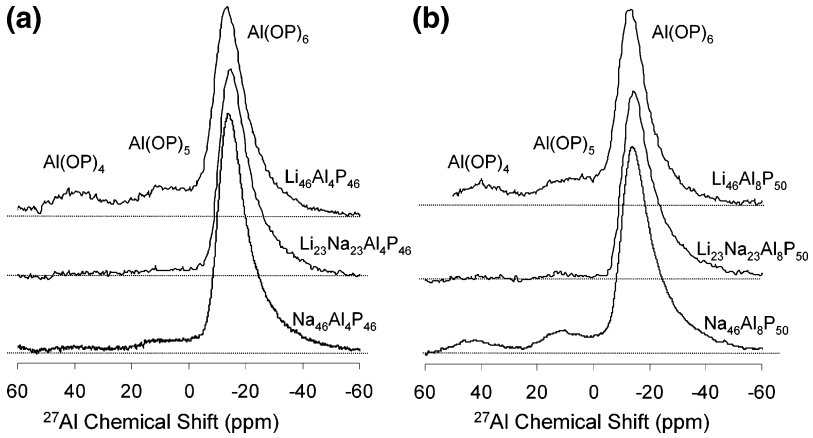

Figure 5. ^{27}Al MAS NMR spectra of (a) 0.46[xNa$_2$O (1 − x)Li$_2$O], 0.50[P$_2$O$_5$], 0.04[Al$_2$O$_3$] and (b) 0.46[xNa$_2$O (1 − x)Li$_2$O], 0.46[P$_2$O$_5$], 0.08-[Al$_2$O$_3$] glasses.

interesting to observe is that this high-frequency contribution is much more important in the aluminophosphate glasses with 4 mol % Al$_2$O$_3$ (from 7 to 31% relative surface area) than in the glasses with 8 mol % Al$_2$O$_3$ (2−5% relative surface area).

^{27}Al MAS NMR. ^{27}Al MAS NMR spectra of the aluminophosphate glass series containing 4 and 8 mol % Al$_2$O$_3$ (Figure 5) all exhibit one dominant peak near −15 ppm and, for certain spectra, two small contributions near +12 and +40 ppm. These results are very similar to those obtained in sodium aluminophosphate glasses of close compositions,[27,28] for which the peaks around −10, +15, and +40 ppm have been attributed, respectively, to six-coordinated (Al(OP)$_6$), five-coordinated (Al(OP)$_5$), and four-coordinated (Al(OP)$_4$).

With ^{27}Al being a quadrupolar nucleus, broadening due to second-order quadrupole effects may hinder the resolution of highly anisotropic sites.[27] Since the spectra reported in Figure 5 are peak maxima, uncorrected from quadrupolar effects, an analysis of the peak areas does not strictly provide site concentrations. However, Brow et al., while recognizing "that the absolute values may be in error an unknown amount because of this problem", assume that "the relative peak areas represent relative peak intensities". The consistency of the peak areas they determined at two field strengths and the agreement among the NMR and X-ray photoelectron spectroscopy (XPS) data support their hypothesis. On the basis of the same assumption, we can observe in a quantitative manner that the peaks associated with five-coordinated (Al(OP)$_5$) and four-coordinated (Al(OP)$_4$) are more important in single than in mixed aluminophosphate glasses, where they are almost not detectable, and that these peaks are also more prominent in the Li rich compositions than in the Na rich compositions (at least for the 4 mol % Al$_2$O$_3$ glasses). This possible "MAE" on the mean coordination number of aluminum is however rather small and almost at the limit of the precision of our measurements. As an Al(OP)$_6$ site induces more POAl cross-links per Al than do Al(OP)$_4$ or Al(OP)$_5$ sites, we should observe an associated effect on the P environment analyzed by ^{31}P NMR. Our ^{31}P NMR results are not precise enough (due to the convolution of the different peaks associated with the different P sites) to correlate results observed on Al sites.

SAXS. SAXS intensities measured in the mixed Na−Li phosphate glasses as a function of the scattering vector (q) are presented in Figure 6. In the low-q range (0.6−6 nm^{-1}), the SAXS intensity is almost constant and the same for all compositions. The slight increase observed as the scattering vector increases is due to the presence of the low-q end of the first sharp diffraction peak (FSDP), or amorphous halo, which

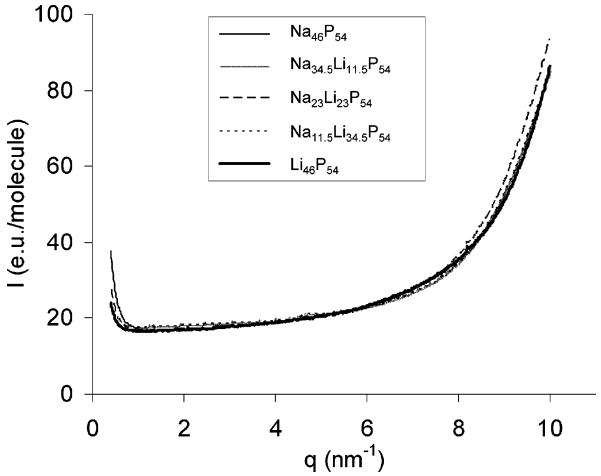

Figure 6. SAXS intensity as a function of scattering vector in the 0.46[xNa$_2$O (1 − x)Li$_2$O], 0.54[P$_2$O$_5$] glasses measured at room temperature.

is clearly visible for q values larger than 8 nm^{-1}. This contribution superimposed on a constant signal whose extrapolation toward $q = 0$ allows determining the amplitude of the thermal density fluctuations in liquids and glasses,[16,29−30] if no other compositional fluctuations contribution alters the signal. We can consequently conclude from Figure 6 that the different Na−Li pure phosphate glasses analyzed here are homogeneous and that the thermal density fluctuations are almost independent of the relative alkali content. There is no evidence for any heterogeneity or segregation region in the mixed alkali glasses.

If we now consider Figure 7, we can observe the influence of alumina incorporation on the long-range order. In the single Na or Li aluminophosphate glasses (Figure 7a and b), we can observe that the spectra show again an almost constant SAXS intensity in the low-q region (up to 6 nm^{-1}) but the level has doubled (from around 20−40 eu/molecule) with alumina incorporation. This indicates that thermal and/or compositional density fluctuations increase when aluminum replaces phosphorus in these single glasses. It is interesting to remark that ^{31}P NMR and SAXS measurements provide evidence for an increase of disorder as alumina is added to the glass, respectively, in the local Q^2_0 environment and in the long-range density fluctuations. In Figure 7, one can also observe that the small-angle intensity is no longer completely flat as a function of q. A very broad maximum around 2 nm^{-1} seems to develop and increase when the Al$_2$O$_3$ content increases. This effect is clearer in the sodium than in the lithium glasses. In the case of the

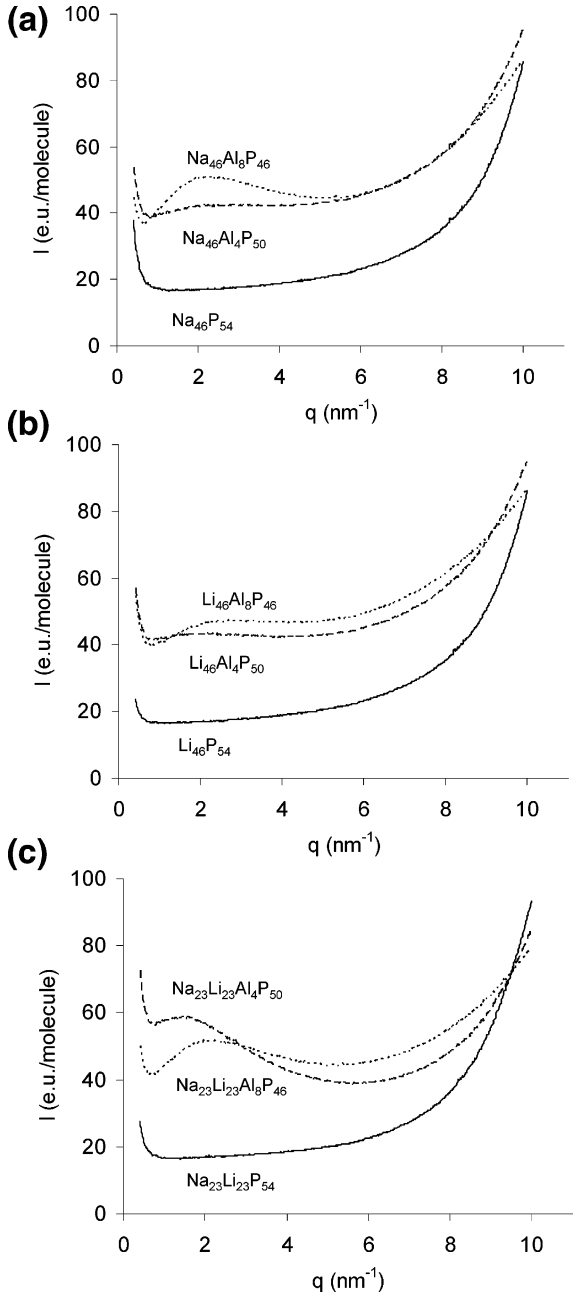

Figure 7. SAXS intensity as a function of scattering vector (a) in 0.46-[Na_2O], 0.54[yAl_2O_3 $(1 - y)P_2O_5$] glasses, (b) in 0.46[Li_2O], 0.54-[yAl_2O_3 $(1 - y)P_2O_5$] glasses, and (c) in 0.46[0.5Na_2O 0.5Li_2O], 0.54[yAl_2O_3 $(1 - y)P_2O_5$] glasses, measured at room temperature.

mixed glasses (Figure 7c), the small-angle correlation peak is much easier to detect. Its maximum appears at q values around 1.5 nm^{-1} for the 4 mol % alumina content and moves to higher q values around 2 nm^{-1} when alumina content reaches 8 mol % (closer to the position determined in the single alkali glasses). Contrary to what happens in the single alkali glasses, the amplitude of the peak decreases with alumina content. Our results reveal that, at least in 4 mol % alumina phosphate glasses, the long-range order is affected by the relative alkali ratio in a nonlinear manner. This is clearly shown in Figure 8. Both the amplitude and the position of the broad correlation peak observed at small angle evolve nonlinearly with the relative alkali ratio. In the 8 mol % phosphate glasses, the results are different: the amplitude and the position of the correlation peak appear to be the same for single or mixed glasses.

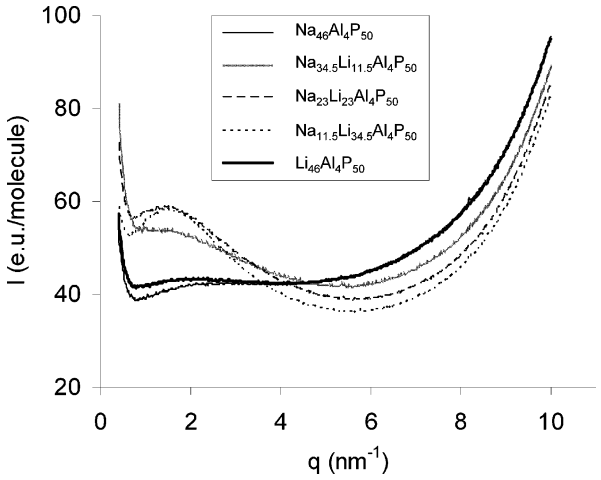

Figure 8. SAXS intensity as a function of scattering vector in the 0.46[xNa_2O $(1 - x)Li_2O$], 0.50[P_2O_5], 0.04[Al_2O_3] glasses measured at room temperature.

Discussion

Most technologically important phosphate glasses contain some aluminum, and the influence of alumina addition to phosphate glasses has consequently been analyzed in the literature. In the case of sodium phosphate glasses, it has been shown that the addition of alumina has significant effects on physical and chemical properties, including raising the glass transition temperature, decreasing the thermal expansion coefficient, and improving the aqueous durability.[31] These changes are in agreement with a general strengthening of the structural network through the formation of POAl bonds. However, for certain properties such as refractive index or density, Al_2O_3 compositional variations present a maximum, suggesting a more complex structural dependence.[31] Brow et al. indeed evidenced that aluminum in sodium phosphate glasses can be either tetrahedrally or octahedrally coordinated and that the [$Al(OP)_6$]/[$Al(OP)_4$] ratio generally correlates with composition/properties changes.[27,28] Zhuravlev et al.[32] note that an $Al(OP)_6$ site provides 50% more POAl cross-links per Al than does an $Al(OP)_4$ site, leading to a more open structure for $Al(OP)_6$ than for $Al(OP)_4$. Brow et al.[27] also observed that octahedrally coordinated aluminum, $Al(OP)_6$, is most abundant in glasses with a low alumina content and more precisely that the average Al coordination number changes from around 6 to around 4 for an [O]/[P] ratio greater than 3.5. The 4 and 8 mol % aluminophosphate glasses have, respectively, [O]/[P] ratios of around 3.08 and 3.26. ^{27}Al NMR results clearly demonstrate that the glasses analyzed here all exhibit a predominant octahedral Al coordinated structure, in agreement with Brow's statement. The addition of alumina in the Na−Li phosphate glasses analyzed here most likely induces the formation of covalently bonded $Al(OP)_6$ species, strengthening the glass network by cross-linking neighboring metaphosphate chains and shortening POP bonds. These conclusions are in agreement with the general increase in elastic Young modulus and in the glass transition previously described as Al_2O_3 is added in these glasses.[15] The shortening of the POP bonds is also revealed by the changes in the isotropic chemical shift measured by ^{31}P NMR for the Q^2_0 species as the alumina content increases (see Figure 4). However, a detailed distribution of these $Al(OP)_6$ species along the phosphate chains is difficult to describe. If we consider a homogeneous distribution of $Al(OP)_6$ octahedra along the phosphate chains, only short, pure phosphate chains should remain. In the glasses with 4 mol % Al_2O_3, the proportion of

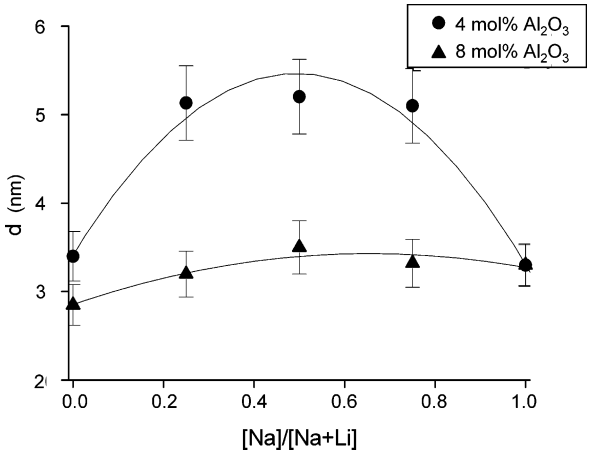

Figure 9. Estimated correlation length ($d = 2\pi/q$) obtained from the small-angle correlation peak appearing in the SAXS spectra, plotted as a function of the relative alkali content of the [xNa$_2$O ($1 - x$)Li$_2$O], 0.50[P_2O_5], 0.04[Al_2O_3] and 0.46[x Na$_2$O ($1 - x$)Li$_2$O], 0.46[P_2O_5], 0.08[Al_2O_3] glasses.

Q^2_0 species should be almost the same as the proportion of Q^1_1 species, and in the glasses with 8 mol % Al_2O_3, only Q^1_1 species should remain. Rather, ^{31}P NMR results indicate a Q^2_0/Q^1_1 ratio higher than 1, even in the 8 mol % Al_2O_3 glasses, suggesting that "quite long" phosphate chains persist. From our ^{31}P NMR results presented in Table 3, if we consider again a homogeneous repartition of the Q^2_0 phosphate species forming phosphate chains with all the same length in the glass, we can estimate that these phosphate chains would be composed of about 10 ± 5 P per chain for the 4 mol % Al_2O_3 glasses and of about 7 ± 1 P per chain for the 8 mol % Al_2O_3 glasses. Al(OP)$_6$ are consequently most likely not homogeneously cross-linked along the phosphate chains. Fits of our ^{31}P NMR results also indicate the presence of a rather large proportion of P tetrahedron with a rather negative chemical shift. As already said, this contribution is difficult to resolve and to attribute, but it is most likely due to P being coordinated to more than one Al, which would be in agreement with an "aggregation" of Al(OP)$_6$ species. ^{31}P NMR results however do not allow us to go much further in this analysis because of the high degree of convolution between the different possible Q^n_m species.

From our SAXS measurements, we observe a general increase in the thermal and/or compositional density fluctuations associated with alumina incorporation, but which is not proportional to the alumina content (Figure 7). A broad and more or less well-defined correlation peak also rises up with a maximum around $1.5-2$ nm^{-1} with alumina incorporation. This correlation peak indicates that a relatively well organized structure develops at the long-range order in the glasses when Al_2O_3 is added to the glass composition. It could be associated with a uniform distribution of heterogeneities, corresponding for example to Al(OP)$_6$ species or aggregations of Al(OP)$_6$ species. This correlation peak could also reveal a long-range "structuration" in the phosphate network due to the presence of alumina. At small angles, the position of a correlation peak cannot be directly related to a correlation length in the structure. The peak position also depends on the shape and on the organization of the "repeating units".[33] In a first approximation, we can however determine a characteristic correlation distance (d) using the well-known $d = 2\pi/q_{max}$ relation, where q_{max} is the wave vector at the peak maximum (see Figure 9). The obtained correlation lengths correspond to rather large distances of $3-4$ nm depending on the glass composition, with the distance being larger for the glasses with 4 mol % Al_2O_3 than with 8 mol % Al_2O_3. Again, if we consider that this correlation length corresponds to the typical distance between Al(OP)$_6$ species homogeneously distributed in the glass, the mean distance between Al(OP)$_6$ species we can calculate from glass composition and density is around 0.93 nm for the glasses with 4 mol % Al_2O_3 and around 0.77 nm for the glasses with 8 mol % Al_2O_3. These distances are $4-5$ times smaller than the distances determined experimentally from SAXS measurements (Figure 9). This may again indicate that there is some aggregation of Al(OP)$_6$ in agreement with our first assumptions from ^{31}P NMR results.

Considering now the structural variation in the three glass series as a function of the relative alkali content, ^{31}P NMR results do not indicate any nonlinear variation in the local P environment, although in aluminophosphate glasses very fine change is difficult to obtain due to the high degree of correlation of the different Q^n_m contributions. Modifications of the ^{27}Al nucleus environment result in distortion of the electric field gradient surrounding the ^{27}Al nucleus and thus lead to second-order quadrupolar line broadening. ^{27}Al MAS NMR data consequently exhibit more clearly perturbative effects of glass composition than does ^{31}P MAS NMR, although only qualitatively. Indeed, the different contributions of ^{27}Al NMR spectra are easier to deconvolute and our results indicate the presence of a very small quantity of Al(OP)$_4$ and Al(OP)$_5$ species in single alkali glasses, whereas, in the mixed alkali glasses, Al(OP)$_6$ only seems to contribute to the ^{27}Al NMR spectra. These results, although at the limit of our measurement precision, would imply that the presence of one or two types of ions in the glass very slightly modifies the mean Al coordination number. This slight decrease of the Al coordination number in single alkali glasses however implies a significant reduction of the number of cross-links available to strengthen the network, probably diminishing the effect of alumina on the single alkali phosphate glass properties.

SAXS measurements also reveal a nonlinear variation of the long-range-order structure, especially visible in glasses with 4 mol % Al_2O_3 (Figure 8). A clear correlation peak rises at lower q range with higher amplitude for the mixed glasses than for the single glasses. This result can be related to the Al coordination which is well defined in the mixed glasses (equal to 6) and slightly more distributed in the single alkali glasses. This could explain a broader correlation peak in the single alkali glasses than in the mixed one. This could also explain a higher correlation distance in the mixed glasses than in the single alkali glasses. The nonlinear variation of Al coordination number with the relative alkali ratio is also observed in the 8 mol % Al_2O_3 phosphate glasses, but SAXS correlation peak position and amplitude are now almost independent of the alkali ratio. For the glasses with 4 mol % Al_2O_3, the clear MAE we obtained on the correlation length estimated from SAXS measurements (Figure 9), which almost disappears in the glasses with 8 mol % Al_2O_3, is thus difficult to relate to any change in the P or Al local environments. Still this "structural MAE" indicates that cations play an important role in the network structuration.

Conclusion

In this paper, we analyzed the local and long-range structure of three series of mixed Na−Li aluminophosphate glasses with the same global alkali content and different Al/P ratio.

^{27}Al NMR measurements indicate that, in these glasses, aluminum is mainly octahedrally coordinated but that the average coordination number is very slightly lower than 6 in single alkali glasses than in the mixed one. Both the ^{31}P NMR

and SAXS results moreover seem to indicate that $Al(OP)_6$ species are not homogeneously distributed along phosphate chains but rather segregated. We indeed observe that "rather long" phosphate chains persist in the glasses, and a smooth correlation peak develops in the SAXS spectra, indicating some structuration of the network at long range. These two techniques also demonstrated that Al_2O_3 incorporation enhanced both disorder on local-order and long-range-order fluctuations.

We also observed for the first time a nonlinear variation with the relative alkali content (so-called MAE) of both the local Al environment (although this effect is very small) and of the long-range organization of glasses containing 4 mol % Al_2O_3. If inhomogeneity regions revealed by SAXS measurements correspond to the segregation of $Al(OP)_6$ species, then this segregation is enhanced by the presence of two types of alkali in glasses with 4 mol % Al_2O_3, suggesting that alkali, if they are known to impose their own environment, also influence the organization of aluminum along the phosphate chains.

To go deeper in the relation between these structural results and the understanding of the typical MAE on conductivity, it would be very interesting to confirm the influence of mixed cations on the detailed structure of the aluminum. Also, a more precise description of the organization of $Al(OP)_6$ species along the phosphate chains could be obtained by heteronuclear correlation NMR experiments (HETCOR).

Acknowledgment. ESRF provided the synchrotron radiation facilities, and we thank J.-P. Simon and J.-F. Bérar for assistance in using the BM02 beamline as well as S. Arnaud and B. Caillot for technical assistance. Many thanks are also extended to Prof. J. Phalippou for fruitful discussions.

References and Notes

(1) Isard, J. O. *J. Non-Cryst. Solids* **1969**, *1*, 235.
(2) Day, D. E. *J. Non-Cryst. Solids* **1976**, *21*, 343.
(3) Ingram, M. D. *Phys. Chem. Glasses* **1987**, *28*, 215.
(4) Greaves, G. N. *J. Non-Cryst. Solids* **1985**, *71*, 203.
(5) Huang, C. D.; Cormack, A. N. *J. Chem. Phys.* **1990**, *93*, 8180.
(6) Huang, C. D.; Cormack, A. N. *J. Chem. Phys*. **1991**, *95*, 3634.
(7) Gee, B.; Eckert, H. *J. Phys. Chem.* **1996**, *100*, 3705.
(8) Gee, B.; Janssen, M.; Eckert, H. *J. Non-Cryst. Solids* **1997**, *215*, 41.
(9) Park, B.; Cormack, A. N. *J. Non-Cryst. Solids* **1999**, *255*, 112.
(10) Swenson, J.; Matic, A.; Brodin, A.; Börjesson, L.; Howells, W. S. *Phys. Rev. B* **1998**, *58*, 11331.
(11) Swenson, J.; Matic, A.; Karlsson, C.; Börjesson, L.; Meneghini, C.; Howells, W. S. *Phys. Rev. B* **2001**, *63*, 132202.
(12) Bunde, A.; Ingram, M. D.; Maass, P.; Ngai, K. L. *J. Non-Cryst. Solids* **1991**, *131*−*133*, 1109.
(13) Maass, P.; Bunde, A.; Ingram, M. D. *Phys. Rev. Lett*. **1992**, *68*, 3064.
(14) Bunde, A.; Ingram, M. D.; Russ, S. *Phys. Chem. Chem. Phys*. **2004**, *6*, 3663.
(15) Faivre, A.; Viviani, D.; Phalippou, J. *Solid State Ionics* **2005**, *176*, 325.
(16) Levelut, A. M.; Guinier, A. *Bull. Soc. Fr. Mineral. Cristallogr*. **1967**, *90*, 445.
(17) Prabhakar, S.; Rao, K. J.; Rao, C. N. R. *Chem. Phys. Lett*. **1987**, *139*, 96.
(18) Bunker, B. C.; Tallant, D. R.; Balfe, C. A.; Kirkpatrick, R. J.; Turner, G. L.; Reidmeyer, M. R. *J. Am. Ceram. Soc*. **1991**, *76*, 1287.
(19) Brow, R. K.; Kirkpatrick, R. J.; Turner, G. L. *J. Non-Cryst. Solids* **1990**, *116*, 39.
(20) Van Wazer, J. R. *Phosphorous and its compounds*; Interscience: New York, 1958; Vols. 1 and 2.
(21) Brow, R. K. *J. Non-Cryst. Solids* **2000**, *263*−*264*, 1.
(22) Sato, R. K.; Kirkpatrick, R. J.; Brow, R. K. *J. Non-Cryst. Solids* **1992**, *143*, 257.
(23) Kirkpatrick, R. J.; Brow, R. K. *Solid State Nucl. Magn. Reson.* **1995**, *5*, 1.
(24) Grimmer, A. R.; Wolf, G. U. *Eur. J. Solid State Inorg. Chem.* **1991**, *28*, 221.
(25) Dollase, W. A.; Merwin, L. H.; Sebald, A. *J. Solid State Chem.* **1989**, *83*, 140.
(26) Belkébir, A.; Rocha, J.; Esculcas, A. P.; Berthet, P. *Spectrochim. Acta, Part A* **1999**, *55*, 1323.
(27) Brow, R. K.; Kirkpatrick, R. J.; Turner, L. T. *J. Am. Ceram. Soc.* **1993**, *76*, 919.
(28) Brow, R. K.; Kirkpatrick, R. J.; Turner, L. T. *J. Am. Ceram. Soc*. **1990**, *73*, 2293.
(29) Wendorff, J. H.; Fischer., E. W. *Kolloid Z. Z. Polym*. **1973**, *251*, 876.
(30) Levelut, C.; Faivre, A.; Le Parc, R.; Champagnon, B.; Hazemann, J. L.; David, L.; Rochas, C.; Simon, J. P. *J. Non-Cryst. Solids* **2002**, *307*−*310*, 712.
(31) Brow, R. K. *J. Am. Ceram. Soc*. **1993**, *76*, 913.
(32) Zhuravlev, Y. F.; Pletnev, R. N.; Dmitriev, A. V.; Slepukhin, V. K.; Lapina, O. B. *Fiz. Khim. Stekla (Engl. Transl.)* **1990**, *15*, 379.
(33) Guinier, A.; Fournet, G. *Small Angle Scattering of X-ray*; John Wiley and Sons: New York, 1955.